Renyi-Entropy based Cascaded Classifier for Diabetic Retinopathy Detection using Retinal Fundus Images

Archana S. Thorat
Department of CSE
Pune Cambridge Senior College, Pune, Maharashtra, India.

Abstract: Diabetic Retinopathy (DR) is a disease that damages retinal blood vessel, and nowadays, the effective diagnosis is lacking because of the uneven and inaccurate classification. Hence, diabetic retinopathy has been addressed as an active in research that seeks the researchers contribution. In this research, an effective Diabetic Retinopathy (DR) detection method is developed for the detection of DR using the retinal fundus image. The DR detection method, proposed renyi entropy-based cascaded classifier is developed using the Renyi-Entropy based Cascaded classifier, which is constructed by cascading the Deep Recurrent Neural Network (Deep RNN), Adaboost classifier, and Support Vector Machine (SVM) classifier. The preprocessed retinal fundus image is subjected to the optic disc and blood vessel segmentation using the binarization, Circle fixing, and morphological Top-Hat transform. From the segments, features are acquired that forms the valuable feature vector, and is fed to the Renyi entropy-based cascaded classifier for the classification. The comparative analysis of the proposed Renyi-Entropy based Cascaded classifier is done based on the metrics, like accuracy, sensitivity and specificity. The proposed Renyi-Entropy based Cascaded classifier provided a maximum accuracy, precision, sensitivity, and specificity of 93.7%, 95%, 95%, and 84.9%, respectively for dataset_1 and 91.2%, 95%, 94.8%, and 69.5% of accuracy, precision, sensitivity, and specificity, respectively for dataset_2.

Keywords: Diabetic Retinopathy, Fundus Images, Renyi-Entropy, cascaded classifier, blood vessel segmentation.

1. Introduction

One of the major causes of blindness is the DR. The DR affects the patient suffering from diabetes by mutilating the patient's retinal blood vessel. The DR is of two types such as Non Proliferative Diabetic Retinopathy (NPDR) and Proliferative Diabetic Retinopathy (PDR) [9]. The NPDR denotes the primary stages of DR which is again classified as Moderate, Mild and Severe stages. The appearance of circular red dots at the blood vessel denotes the mild stage of DR which is also known as micro-aneurysm (MA). The further rupture of MAs into deep layers formed a hemorrhage in the retina. The hemorrhage is flame shaped and this denoted the moderate stage of DR. In the severe stage of DR, abnormalities occurred in the intraretinal microvascular along with the bleeding of venous. The PDR is the advanced stage of DR in which the functional microvascular networks known as, neovascularization is formed in the new blood vessels that is present in the surface of the retina. This process of formation of new blood cells made the detection process of the DR in mild stage into a difficult task [10]. By 2025, it is predicted that the patient with DR would increase from 382 million to 592 million [11] [5].

The early stages of DR are mostly asymptomatic but it also has symptom, such as distortions, floaters, blurred vision and progressive visual acuity loss in the advanced stages. Thus, the worse effect in the advanced stage is overcome by detecting the DR at the primary stages. Highly trained domain experts are used for the manual analysis which makes them expensive in terms of cost and time. The manual analysis increased the cost and time required for the analysis which is overcome by the computer vision methods. The computer vision method helps in assisting the physicians for analyzing the images. The computer vision based methods are classified into hand-on engineering [3] and end-to-end learning [12]. The traditional methods, like SIFT [14], HoG [13], Gabor filters [16], and LBP [15] are used for the extraction of the features in the hand-on engineering methods. The limitation in the hand-on engineering method is encoding the variations during the rotation and illumination. In the case of end-to-end leaning, the rich features that are hidden are learned automatically for performing better classification. Although

the end-to-end learning based methods and the hand on engineering methods detected the DR, it failed to detect the Mild stage of DR [5].

The early diagnostic is necessary for the optimal treatment of the DR and hence, the regular examination of eye. Most communities did not provide the continuous follow-up and the frequent consultations that are required for screening [17]. Hence, the underserviced populations are reached by the management of DR. In the recent researches, the issues related to Computer-Aided Diagnosis are taken into consideration. Most existing researches are related to the DR lesion detection that uses the visual characteristics that are specific to each lesion type [20]. A few unified DR-lesion detectors are developed recently which is much harder to automatically decide whether or not to refer the patient to the ophthalmologist [19]. The assessment of risk in DR is based on the presence and evolution of lesions, subtle hints that are revealed during the anamnesis and examination. The semi automated or automated decision of the referable cases reduced the workload of the specialist whilst attending the patients in need. In order to serve the patients better, the high-risk cases should be prioritized for isolated, poor, or rural communities [18]. At present, the DR-lesion classifiers are combined into final decision for providing automated referral decisions. These models has limited accuracy and difficult to implement. For accessing the referability of the patients directly, various methods based on the maximum-margin support vector machine (SVM) classifiers and the Bags of Visual Words (BoVW) model is considered. The advanced mid-level features, like Fisher Vector and Bossa Nova are used for improving the referral assessment for extending the BoVW model [2].

The main contribution of the research is modeling a classification strategy based on the optimization algorithm. Initially input image is pre-processed which is followed by the detection of optic disc. The optic disc is detected using the Circle fixing and binarization methods. Subsequently, morphological Top-Hat transform is applied on the pre-processed image for the segmentation of the blood vessels. After that, the feature like standard deviation, variance, mean, kurtosis and energy are extracted from the blood vessels and the optic disc respectively. In addition to these features, the CNN features obtained from the input image is also included for formulating the feature vector. Finally, the features are classified using Renyi entropy-based cascaded classifier.

The organization of the research are as follows, section 1 introduces the Diabetic Retinopathy, section 2 explains the literature review and the challenges of the existing Diabetic Retinopathy classification methods, section 3 discusses the

2. Motivation

This section explains the literature review of the DR detection techniques. Eight existing methods of DR detection and the challenges of the DR detection methods are discussed.

2.1 Literature Review

The existing methods of the DR detection along with the disadvantages are as follows,

Zeng, X. et al. [1] developed a deep learning algorithm for the detection of DR. In this method, the binocular fundus images are taken as the input and the pathological correlation of the eyes were used for predicting the possibility of Diabetic Retinopathy. Although this method had high sensitivity and AUC, it failed to implement the techniques in large sets of data. Pires, R. et al [2] designed a DR-lesion detection method. In this method, classifier was directly trained for the DR referral. Although this method provided better results for referral assessment, it failed to investigate the automated decision in terms of DR progression. Seoud, L.et al.[3] modeled a Dynamic Shape Features (DSF) for the detection of Red lesion detection method. The DSF features did not require the accurate segmentation of the region. This method was robust and they were highly capable of discriminating between the segments of the vessels and lesions. However, this method failed to focus on the bright and neovessel detection of lesion. Zhou, L. et al.[4] developed a deep MIL method for the lesion detection. The patch-level estimation of DR was achieved by deeply fine tuning the pre-trained AlexNet. The irregular DR lesions were handled using the end-to-end multi-scale framework. Although this method improved the detection performance, it failed to implement the active learning and semi-supervised learning techniques.

Qummar, S.et al.[5] designed a Deep Learning Ensemble method for the detection of DR. This method detected and classified the different stages of DR accurately using the CNN ensemble-based framework. However, this method had reduced accuracy for the early stages and the underlying complicated features were unable to encode. Costa, P.et al.[6] modeled a Multiple Instance Learning (MIL) framework for the detection of DR. Based on the implicit local information, the presence of DR was predicted. The classification stages and encoding were connected through the joint-learning scheme. Although this method had improved detection accuracy for the detection of DR, it failed to detect the

different levels of DR. Gao, Z.et al.[7] developed a DR detection method using Deep Neural Networks. In this method, the fundus image was changed into uniform format using preprocessing pipeline. This method provided pilot diagnostic services to the hospital by deploying the model on the cloud computing platform. Although this method provided better consistency rate, it failed to use the accumulated data for improving the accuracy and include the data from different equipments. De la Torre, J. et al.[8] designed a Deep Learning Interpretable Classifier for the detection of DR. The pixel contribution to the classification was indicated in terms of scores. A pixel-wise score propagation model was developed for obtaining the scores. The underlying statistical regularities were found by generating the visual maps. However, this method failed to create manually marked lesions as it lacks the Radial Diffusivity images.

In 2023, Soares*et al.* [29] have implemented a multi-scale algorithm for the detection of microaneurysms automatically. Initially, images were pre-processed to their required size and contrast. Using the multi-scale algorithm, the microaneurysm and rental vessels were detected. The microaneurysm was extracted using various scales such as hessian-based blob and top-hat filter detectors. Then retinal vessels from the images were removed through a multi-scale line filter. The multi-scale approach was used to identify the microaneurysm images and healthy images and they were represented as True and False. Moreover, they also detect microaneurysms based on their size and also contrast. Finally, the result was then evaluated and compared with existing methods and obtained promising results.

In 2023, Thanki *et al.* [30] have executed an intelligent computer-aided triage system. Initially, in this method fundus retinal images were taken as inputs. The features of the images were separated using DNN and classified into various categories through an ML classifier. Then the performance of each classifier was analyzed and found that the logistic regression classifier performed well than other classifiers. The classifier classifies images into normal and glaucomatous images using a two-fold cross-validation method.

In 2023, Palaniswamy, T. and Vellingiri, M., [31] have adopted DL and IoT for the detection of DR using retinal fundus images. Initially, data was collected through IoT Devices and they were transferred through a cloud server for further processing. The noise from the images was removed and the images were enhanced in the preprocessing stage. The mayfly optimization-based region growing (MFORG) technique was used for lesion segmentation in the fundus images to accurately detect the lesion regions in the fundus images. Furthermore, the images were feature extracted, classified and parameters were optimized for evaluation. Finally, the result showed more accurate results than the existing method.

In 2023, Sahoo *et al.* [32] have compared the performance of the two standard databases through lesion identification techniques. Initially, DIARETDBO and DIARETDB1 were used as the standard datasets. The input data was preprocessed through four methods. The image was then segmented based on various categories. Then the blood vessels in the images were removed and features were extracted. Furthermore, the data were prepared for transformation and then it was classified through various approaches to get the expected output. Finally, the output was validated and compared with an existing method to update accurate results.

In 2023, Luo *et al.* [33] have implemented DL method through LRU and trained networks. Initially, the photograph of the fundus was used as an input to the DL network. The CNN architecture was used to separate the features in the images, where images were divided into feature maps into patches that were compared with the other patches. The similarities of the patches were compared and calculated through the gaussian function. In addition to this, similarity weights were computed as the sum of all weighted patches in the feature map. The use of a large-range unit with a residual structure incorporated a correlation between long-range patches in the DL framework. Finally, the output was trained and tested with a Long-Range unit and various datasets were evaluated and the performance was obtained. The result was effective to detect DR accurately.

In 2023, Gu *et al.* [34] have classified DR through Feature Extraction Block (FEB) and Grading Prediction Block (GPB). Initially, the input images enhanced their contrast and removed noise through preprocessing. The features were extracted through FEB. It also used a transformer that focuses mainly on exudate areas and the retinal hemorrhage. After that, GPB classifies the DP in five stages where it captures different spatial region that was occupied through various classes of objects. The loss function was also used to optimize the model during training and performance was evaluated through DDR dataset and output were obtained.

In 2023, Bajwa *et al.* [35] have adopted the DL model to detect DR in the early stage. Initially, this model contains a training and validation phase and a testing phase. Initially, the data were collected and labeled as Positive or Negative DR by an expert. It was also further divided into training and validation datasets that were used as the input for CNN to validate and train the results. The output from CNN was featured as an active map and pooling was performed. In the testing phase, the real-time dataset from Type-II diabetics patients was used as input. Finally, the inputs were evaluated and reviewed

through exerts to evaluate the performance and compare the results with trained models. This method helped in the early detection of DR and prevent losing sight.

In 2023, Jena*et al.* [36] have used the DL method for DR screening. Initially, this method used contrast-limited adaptive histogram equalization (CLAHE) was used for image enhancement. The image was segmented into the optic disc and blood vessels through U-Net. The CNN and SVM were further used for classification where it was classified into four classes. Finally, the results were tested with the other two data sets and the output was obtained. This method outperformed other existing methods and provided accurate results.

2.2. Challenges

The challenges faced during the implementation ofDiabetic Retinopathy are as follows,
- The annotated training data in the MIL framework ranges were medium to moderate and labeling the image regions in each pixel with the lesions manually were aerror-prone and time-consuming process [6].
- In [5], the Deep Learning Ensemble method detected the stages of DR but the main challenge lies in improving the accuracy for the early stages and the encoding the underlying complicated features.
- In [2], although the DR-lesion detection method reduced the error during classification, the representation of the image needs to be improved for accurate diagnosis [2].
- The Red lesion detection method based on Dynamic Shape Features (DSF) had the capability of discriminating the lesions segment and the vessels but the main challenge was the detection of the bright lesion and neo vessel [3].
- In the deep MIL method, the challenge lies in the implementation of active learning and semi-supervised learning for the accurate segmentation of DR lesions [4].

3 Diabetic Retinopathy Detection Method using the Renyi Entropy based Cascaded Classifier

This section describes the proposed DR detection method that enables the effective detection of DR. Initially retinal fundus image is pre-processed for further processing which is followed by the segmentation of the blood vessel and the detection ofoptic disc. The optic disc is detected using the Circle fixing and binarization methods. Subsequently, morphological Top-Hat transform is applied on the pre-processed image for the segmentation of the blood vessels. After that, the feature like standard deviation, variance, mean, kurtosis and energy are extracted from the blood vessels and the optic disc respectively. In addition to these features, the CNN features obtained from the input image is also included for formulating the feature vector. Finally, the features are classified using Renyi entropy-based cascaded classifier. The cascaded classifier is constructed using Deep Recurrent Neural Network (Deep RNN), Adaboost classifier, Support Vector Machine (SVM).Fig.1 shows the block diagram of the DR detection method using the Renyi entropy based cascaded classifier.

.
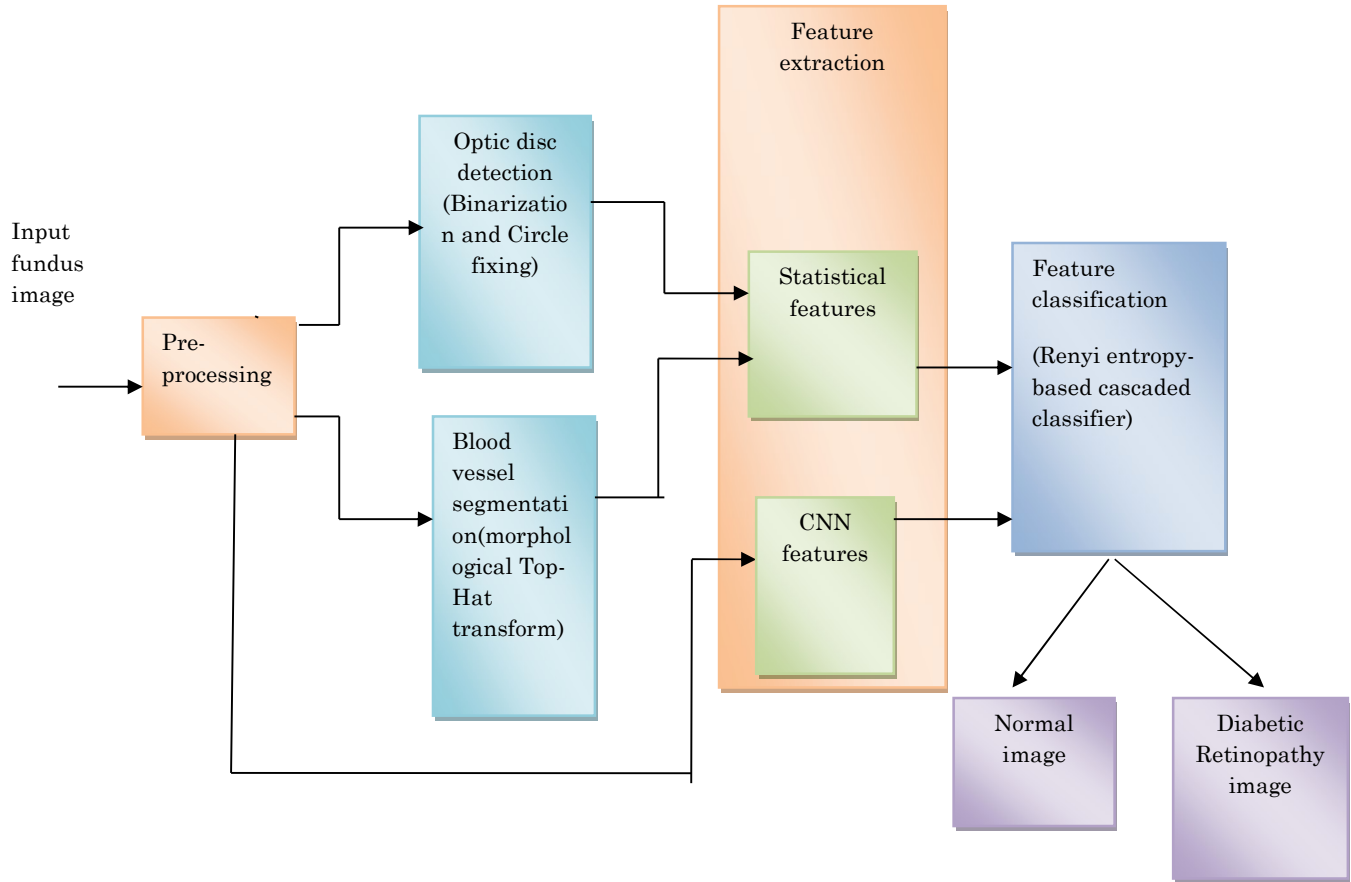
Fig.1. *Block diagram of the proposed Diabetic Retinopathy detection method*

Let us assume the database $\overline{D}$ with t retinal fundus image and is given as,

$$\overline{D} = \left\{ \bar{I}_1, \bar{I}_2, ..., \bar{I}_k, ..., \bar{I}_t \right\} \tag{1}$$

where, the kth input image is represented as, $\bar{I}_k$ and the total number of images is represented as, t.

3.1. Pre-processing of Input Image

The input image is pre-processed for making it appropriate for the DR detection process. In Pre-processing, the noise in the image is eliminated and makes the input image suitable for smoother processing. The image contrast can be enhanced further by the pre-processing step for effective DR detection. After pre-processing, the image is passed to the blood vessel detection module and the optic disc detection module for the extraction of the features that are significant.

3.2. Segmentation of the Optic disc using Binarization and Circle Fitting Techniques

After the pre-processing, the optic disc is detected. The detection of the optic disc is based on the circle fitting and binarization techniques [22]. When compared to other image regions, the optic disc region poses hard exudates, high intensities and sharp boundaries. The glaucomatous region is found by determining the optic disc.

i) Binarization
In the binarization technique, the smooth textures in the pre-processed image are used for the optic disc detection. The smoother regions as well as the complicated regions are separated by considering the values of the pixels. The binarization methods convert the grey scale image that ranges from 0 to 256 into black and white image that can be either 0 or 1. Based on the pixel value, set of images are generated from the results from two classes, whereas the mean value of the entire pixel is used for assigning the value of pixel, which is either 0 or 1. For the greater mean value and lower mean value, the value of the pixel is represented as 1 and 0, respectively. The binary images are generated by thresholding process. If the threshold value is lower than the value of the pixel then, the pixel value is given as 1 and if the threshold is higher than the value of the pixel, the pixel is given as 0. Lastly, the

pixel is filled with black or white color depending on the label of the pixel for the construction of the binary image.

ii) Circle fitting
The circle fitting is the process of fitting the circle around the optic disc region. The normal and glaucomatous retinal images are detected by classifying the image using the optic disc shape. The attributes considered in the optic disc while circle fitting are,
- The radius of the circle (R)
- The x-co-ordinate of circle (X)
- The y-co-ordinate of circle (Y)

3.3. Segmentation of the Blood vessel using Morphological Top-Hat transform

The morphological top hat transform plays a major role by providing information regarding the structure of the blood vessel in the segmentation of the blood vessel. In the morphological top hat transform, the operations, like erosion and dilation are used for the segmentation. The morphological operators apply the structuring elements to the binary images. The segmentation of the blood vessel using the morphological top hat transform is given as,

$$M_T = I - (I \bullet M) * N \tag{2}$$

where, I is the image of the input green channel and SC and SO are closing operator's and opening operator's structuring elements, the closing and opening operators are denoted as '∘' and '∗' respectively.

3.4. Extraction of the Features from the Blood vessels, Optic Disc, and the input Fundus Image

The effective DR detection is performed by the extraction of features, like image level and the blood vessel features. The features, such as mean, variance, energy, kurtosis are extracted from the blood vessel and optic disc. In addition to the statistical features, CNN features are extracted directly from the input image. The features are described below,

a) Mean: The average of the image pixels is defined as mean. The mean is determined as,

$$s_1 = \frac{1}{|c(R_n)|} \times \sum_{n=1}^{|c(R_n)|} c(R_n) \tag{3}$$

where, the mean of the image pixels is represented as, s_1, the total segments is denoted as, n, pixel value of each segment and the total pixel in the segment is indicated by $c(R_n)$ and $|c(R_n)|$.

b)Variance: The variance is determined by the below expression,

$$s_2 = \frac{\sum_{n=1}^{|c(R_n)|} |R_n - \overline{\mu}|}{c(R_n)} \tag{4}$$

where, s_2 represents the variance of the image pixels.

c) Kurtosis: The sharpness of the peak that describes the evenness is termed as, Kurtosis. The kurtosis of the image pixels is represented as, s_3.

d) *Standard deviation:* The square root of the variance is the standard deviation. The standard deviation in the image pixels is represented by the term s_4.

e) Energy: The energy of all the pixels in the segment is summed to extract the energy of the individual segments. The energy of the image pixels is determined as,

$$s_5 = \sum_{n=1}^{|c(R_n)|} c(R_n) \tag{5}$$

where, s_5 denotes the energy feature of the image pixels.

f) *CNN features:* The complex features from the segmented image are extracted using the CNN architecture which contains a multilayered network. The CNN architecture consists of three different layers, like pooling layer, convolution layer and the fully connected layer. The features are extracted from the segmented image in the convolution layer, which is the first layer of the architecture. The relation between the pixel values and the image features are preserved in the first layer. The output from the segmented image is given as the input to the convolution layer. In the convolution layer, the CNN features are extracted. The feature is termed as CNN because it is extracted at the first convolution layer. The CNN feature has the dimension of $[1 \times 256]$ and it is represented as, s_6.

3.4.1. Formation of Feature Vector

The feature from the input image, blood vessel and the optic disc are extracted to form a feature vector which is given as,

$$B = \{s_1, s_2, s_3, s_4, s_5, s_6\} \tag{6}$$

The feature vector formed is given to the RNN classifier for classifying the images based on the derived class label and the provided features. The classifier derives the class label, which is followed by the classification of the input image into normal and DR image.

3.5 Proposed Renyi Entropy based cascaded Classifier for Feature Classification

This section describes the DR detection method using the proposed Renyi entropy based cascaded classifier. The input to the proposed Renyi entropy based cascaded classifier is th feature vector obtained from the features. The proposed Renyi entropy based cascaded classifier is formed by cascading the DeepRNN, Adaboost classifier and the SVM classifier through renyientropy. The Renyi entropy based cascaded classifier classifies the image as normal and DR image depending upon the features extracted from the blood vessels and optic disc. The output of the Renyi entropy based cascaded classifier is represented as,

$$O = \lambda C_1 + \sigma C_2 + \rho C_3 \tag{7}$$

where, O is the output from the Renyi entropy based cascaded classifier, λ is the Renyi entropy of the output of C_1 and target output. σ is the Renyi entropy of the output of C_2 and target output and ρ is the Renyi entropy of the output of C_3 and target output. Below is the description of the classifiers mentioned in equation (7).

3.5.1. DeepRNN for the Classification of Features

The deep RNN is a Elman-type network that connects the internal layers in the time direction at the same hierarchy. At time g, the input vector of the rth layer is given as, $u^{(r),g} = [u_1^{(r),g} u_2^{(r),g} \dots u_q^{(r),g} \dots u_q^{(r),g}]^V$ and the output vector of the rth layer is given as, $y^{(r),g} = [y_1^{(r),g} y_2^{(r),g} \dots y_q^{(r),g} \dots y_q^{(r),g}]^V$. The unit is defined as the pair of the elements in the input and the output vectors, the total number of units is denoted as, J and the arbitrary unit number of the rth layer is denoted as, j. Let us assume that in the output layer $z^g = y^{(1),g}$ and in the input layer $a^g = u^{(C),g}$ and $x^g = y^{(C),g}$. At the layer, the arbitrary unit number is represented as, i (and T, respectively). The propagation weight of the input from the $(r-1)^{th}$ to r^{th} layer is denoted as, $L^{(r)} (\in J^{U \times T})$. In the rth layer, the recurrent weight is denoted as, $H^{(r)} (\in J^{U \times U})$, where the arbitrary unit number of the rth layer is given as, j'. The components of $u^{(r),g}$ is given by,

$$u_j^{(r),g} = \sum_i^I h_{ji}^{(r)} y_i^{(r-1),g} + \sum_{j'}^J d_{jj'}^{(r)} y_{j'}^{(r),g-1} \tag{8}$$

where the elements of $L^{(r)}$ and $H^{(r)}$ are represented as, $h_{ji}^{(r)}$ and $d_{jj'}^{(r)}$ respectively. At the rth layer, the elements of the output vector is represented as,

$$y_j^{(r),g} = f^{(r)}(u_j^{(r),g}) \tag{9}$$

where, the activation function is given as, $f^{(r)}(.)$, $f(u) = \tanh(u)$ and $f(u) = 1/(1+e^{-u})$ are the sigmoid and the logistic sigmoid function, and $f(u) = \max(u,0)$ is the function of the rectified linear unit (ReLU). The 0-th unit $h_{j0}^{(r)}$ and the 0-th weight $y_0^{(r-1),g}$ are introduced for simplicity. The biases are given as,

$$y^{(r),g} = f^{(r)}\left(L^{(r)} y^{(r-1),g} + J^{(r)} y^{(r),g-1} \right) \qquad (10)$$

where, $f(l) = [f(l_1) f(l_2)...f(l_H)]^V$. The output of the arbitrary time is obtained by shifting the value in the above equation. As there is no recurrent connection in the elements of a^g. The output vector at the output is defined as,

$$x_g = f^{(C)}(a^g) = f^{(C)}(L^{(C)} y^{(c-1),g}) \qquad (11)$$

The output from the Deep RNN is represented as, C_1.

3.5.2. Adaboost classifier for the Classification of Features

The Adaboost classifier constructed the strong classifier as the linear combination to weak classifiers [28]. A set of training data, $(\bar{u}_1, v_1)...,(\bar{u}_p, v_p)$ is considered as the input, where the label $v_i \in \{-1,1\}$ and $\vec{u}_i$ is a w-dimensional feature vector. The classifier is run V times (rounds) by the AdaBoost. The integer V generalizes well to the non-training data and did not overfit. The distribution weight on the training data is given as $G_\tau(i)$, where the round index is denoted as, τ. All the weights are equal $(G_\tau(i) = 1/p)$ at the outset $V = 0$. The misclassified pixel weights are increased at each round. The weak hypothesis, $\{\bar{u}_1,...,\bar{u}_p\} \to \{-1,1\}$ suitable for the distribution $G_\tau(i)$ is found by the weak learner.

For all the features, the possible thresholds are checked by the weak learner algorithm while searching for k_τ. The learner algorithm working at the fixed feature j is given as, $(j = 1,...,w)$. The error is calculated for ensuring the goodness of the weak hypothesis,

$$b_\tau = \sum_{i:k_\tau(\bar{u}_i) \neq v_i} G_\tau(i) \qquad (12)$$

The weights G_τ are updated by choosing the parameter, $\beta_\tau = \frac{1}{2}\ln((1-b_\tau)/b_\tau)$ using the following update rule,

$$G_{\tau+1}(i) = \frac{G_\tau(i)}{S_\tau} \times \begin{cases} \exp(-\beta_\tau); & \text{if } k_\tau(\bar{u}) = v_i \\ \exp(\beta_\tau); & \text{if } k_\tau(\bar{u}) \neq v_i \end{cases} = \frac{G_\tau(i)\exp(-\beta_\tau v_i k_\tau(\bar{u}_i))}{S_\tau} \qquad (13)$$

where, the normalization factor S_τ is chosen such that $G_{\tau+1}$ is a distribution function. The correctly classified example's weight is decreased and the example's misclassified weight is given by k_τ which is increased using the update rule. The final updated classifier is as follows,

$$D(u_i) = \text{sign}\left(\sum_{\tau=1}^{V} \beta_\tau k_\tau(\bar{u}_i) \right) \qquad (14)$$

The weight of the weak classifiers is combined together to form a final strong classifier. The class (non-pixel and pixel) was decided by applying the threshold to the output. The receiver operating characteristics (ROC) curves are used for the determination of the threshold value. The output of the Adaboost classifier is given as, C_2.

3.5.3. SVM for the Classification of Features

SVM constructs the optimal hyperplane by seperating both the classes with the largest margin [21]. The generalization error is minimized depending upon the principle of structural risk minimization (SRM) induction [26]. For classifying the unknown point $\bar{x}$, the decision function for the optimal hyperplane $e.\bar{x} + o = 0$, $o \in N$ and $e \in N^R$ is represented as,

$$f(\bar{x}) = \text{sign}(e\bar{x} + o) = \text{sign}\left(\sum_{i=1}^{n_s} \eta_i \bar{x}_i \bar{x} \right) \qquad (15)$$

where, the support vector and the support vector number is denoted as, S_N and $\bar{x}_i$. The Lagrange multiplier is represented as, η_i and the class $\bar{x}$ belongs to $\tilde{m}_i \in \{-1,+1\}$.

The hyperplane suitable for the process is constructed by mapping the input space with the higher dimensional feature space. The feature vector is considered from N^R to a feature space Y for mapping μ. The dot product is computed using the kernel function in the feature space that uses the points in the input space, which is

$$\overline{z}_i \cdot \overline{z}_j = \omega(\overline{x}_i)\,\omega(\overline{x}_j) = K(\overline{x}_i\,\overline{x}_j) \qquad (16)$$

where, $K(.,.)$ is the kernel function. At last, the decision function is converted as,

$$f(\overline{x}) = \text{sign}\left(\sum_{i=1}^{n_S} \eta_i \widetilde{a}_i\, K\left(\overline{x}_i, \overline{x}\right) + o \right) \qquad (17)$$

The kernel functions satisfied the Mercer's theorem and it includes the polynomial, linear kernel and radial basis kernel, etc. The output from the SVM classifier is represented as, C_3.

4. Result and Discussion

The result and analysis of the proposed proposed Renyi-Entropy based Cascaded Classifier is discussed in this section. The enaluation metrics, like accuracy, sensitivity, specificity, precision and TPR.

4.1 Experimental Setup

The proposed Renyi-Entropy based Cascaded Classifier is implemented in MATLAB having Windows 10 OS and 2GB RAM.

4.1.1. Experimental Results

a)

b)

c)
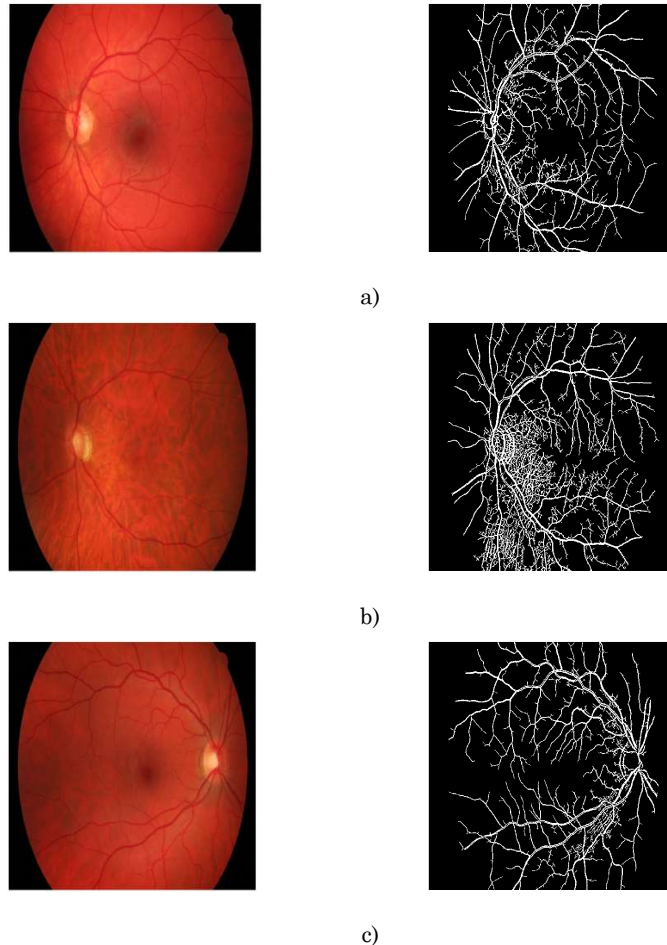
Fig.2. *Experimental results of a) normal image and its segmented output b&c) DR affected image and its segmented output*

Fig. 2. Experimental results of the normal image and DR affected image. Fig. 2 a) Experimental results of the normal image and its segmented image. Fig. 2 b) Experimental results of the DR affected image and its segmented image. Fig. 2 c) Experimental results of the DR affected image and its segmented image.

4.2. Dataset Description

The dataset used for the experimentation are the DIARETDB0 database [23] and DIARETDB1 database [24].

Dataset_1: The DIARETDB0 database of 130 color fundus images. Out of 130 images, 20 images are normal and 110 images are DR images. The images are captured in a unknown camera settings using the 50 degree field-of-view digital fundus camera. This data is also known as, "calibration level 0 fundus images".

Dataset_2: The DIARETDB1 database consists of 89 color fundus images. Out of 89 images, 5 images are normal and 84 images contain mild non-proliferative signs of DR. The images are captured in a different image settings with a 50 degree field-of-view digital fundus camera. The data base is also known as "calibration level 1 fundus images".

4.3. Competing Methods

The competing methods, such as Multiple Instance Learning [4], Ensemble [5], Adaboost classifier [28], and Deep Neural Network [7] are compared with the proposed Renyi-Entropy based Cascaded Classifier for the detection of DR.

4.4 Performance Metrics

The comparative analysis of the proposed Renyi-Entropy based Cascaded Classifier is used for the evaluation of the metrics, like accuracy, sensitivity, specificity, precision and TPR

4.4.1 Comparative analysis using dataset_1
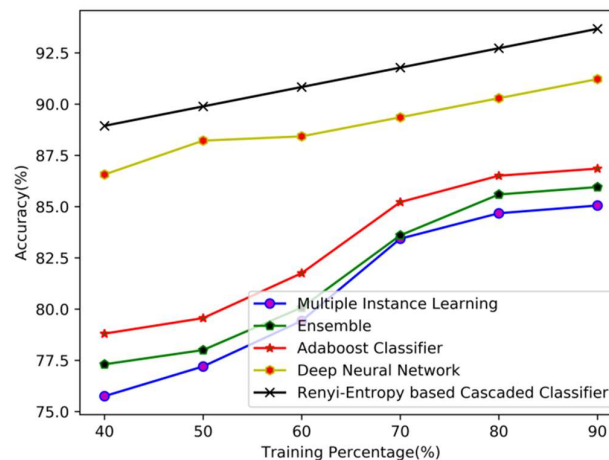
Fig.3. *Comparative Analysis using Accuracy*

Fig.3 shows the comparative analysis using accuracy with respect to the training percentage. When the training percentage is 40, the accuracy obtained by the existing Multiple Instance Learning, Ensemble, Adaboost classifier, Deep Neural Network and the proposed Renyi-Entropy based Cascaded classifier are 75.8, 77.3, 78.8, 86.6 and 88.9, respectively. The accuracy obtained by the existing Multiple Instance Learning, Ensemble, Adaboost classifier, Deep Neural Network and the proposed Renyi-Entropy based Cascaded classifier for the training percentage of 60 is 79.4, 80.1, 81.8, 88.4, and 90.8, respectively. When the training percentage is 90, the accuracy obtained by the existing Multiple Instance Learning, Ensemble, Adaboost classifier, Deep Neural Network and the proposed Renyi-Entropy based Cascaded classifier are 85, 85.9, 86.8, 91.2, and 93.7, respectively.
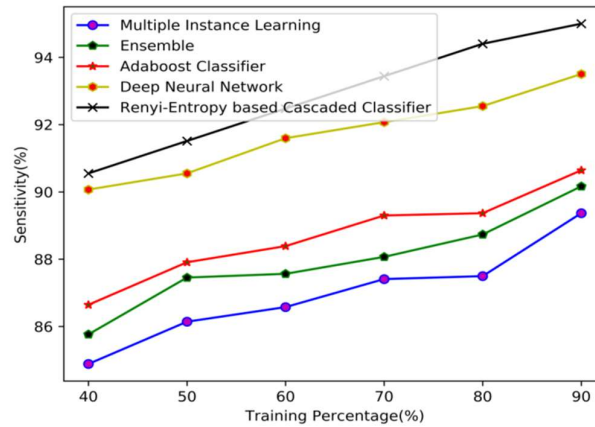
Fig.4.*Comparative Analysis using Sensitivity*

Fig.4 shows the comparative analysis using sensitivity with respect to the training percentage. The sensitivity obtained by the existing Multiple Instance Learning, Ensemble, Adaboost classifier, Deep Neural Network and the proposed Renyi-Entropy based Cascaded classifier for the training percentage of 40 is84.9, 85.8, 86.6, 90.1, and 90.6, respectively. When the training percentage is 60, the sensitivity obtained by the existing Multiple Instance Learning, Ensemble, Adaboost classifier, Deep Neural Network and the proposed Renyi-Entropy based Cascaded classifier are 86.6, 87.6, 88.4, 91.6 and 92.5, respectively. The sensitivity obtained by the existing Multiple Instance Learning, Ensemble, Adaboost classifier, Deep Neural Network and the proposed Renyi-Entropy based Cascaded classifier for the training percentage of 90 is89.4, 90.2, 90.6, 93.5 and 95, respectively.
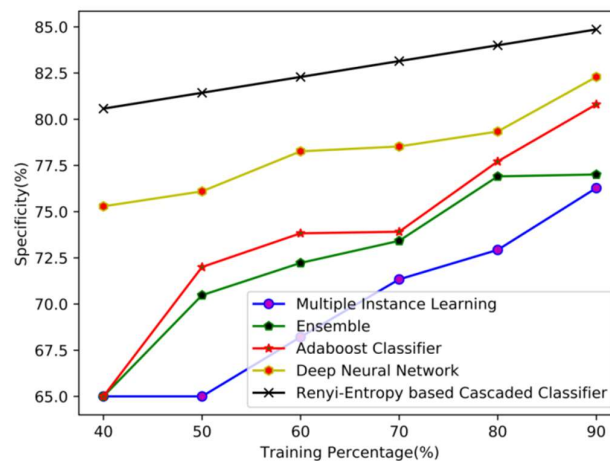
Fig.5.*Comparative Analysis using Specificity*

Fig.5 shows the comparative analysis using specificity with respect to the training percentage. When the training percentage is 40, the specificity obtained by the existing Multiple Instance Learning, Ensemble, Adaboost classifier, Deep Neural Network and the proposed Renyi-Entropy based Cascaded classifier are 65, 65, 65, 75.3 and 80.6, respectively. The specificity obtained by the existing Multiple Instance Learning, Ensemble, Adaboost classifier, Deep Neural Network and the proposed Renyi-Entropy based Cascaded classifier for the training percentage of 60 is 68.2, 72.2, 73.8, 78.3 and 82.3, respectively. When the training percentage is 90, the specificity obtained by the existing Multiple Instance Learning, Ensemble, Adaboost classifier, Deep Neural Network and the proposed Renyi-Entropy based Cascaded classifier are 76.3, 77, 80.8, 82.3 and 84.9, respectively.
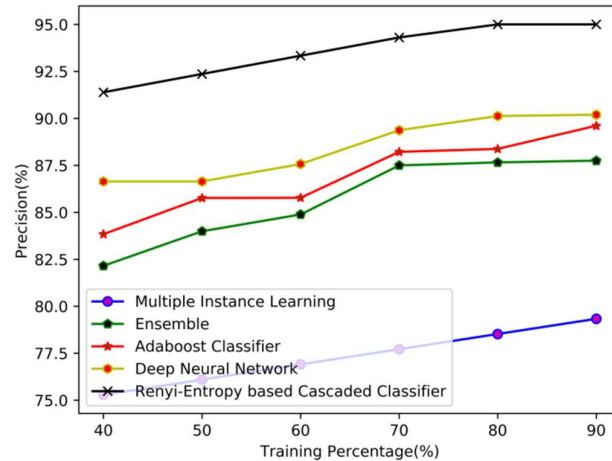
Fig.6.*Comparative Analysis using Precision*

Fig.6 shows the comparative analysis using precision with respect to the training percentage. The precision obtained by the existing Multiple Instance Learning, Ensemble, Adaboost classifier, Deep Neural Network and the proposed Renyi-Entropy based Cascaded classifier for the training percentage of 40 is 75.3, 82.2, 83.8, 86.6 and 91.4, respectively. When the training percentage is 60, the precision obtained by the existing Multiple Instance Learning, Ensemble, Adaboost classifier, Deep Neural Network and the proposed Renyi-Entropy based Cascaded classifier are 76.9, 84.9, 85.8, 87.6 and 93.3, respectively. The precision obtained by the existing Multiple Instance Learning, Ensemble, Adaboost classifier, Deep Neural Network and the proposed Renyi-Entropy based Cascaded classifier for the training percentage of 90 is 79.3, 87.8, 89.6, 90.2 and 95, respectively.
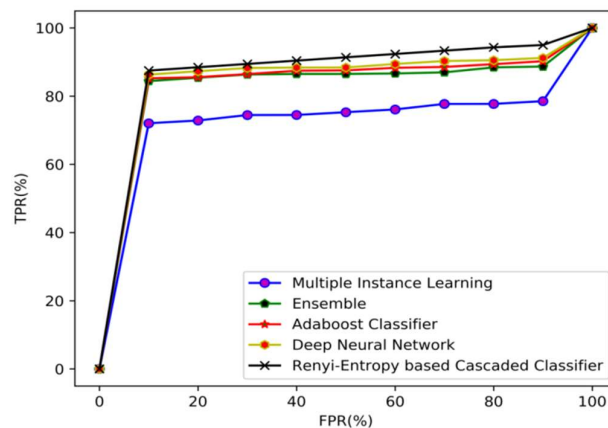
ROC curve:

Fig.7. *ROC curve of Dataset_1*

Fig.7. shows the ROC curve of dataset_1. The comparative analysis of the proposed Renyi-Entropy based Cascaded classifier with the existing methods in terms of True positive rate (TPR) with respect to the False Positive rate (FPR). When the FPR is 20%, the TPR obtained by the existing Multiple Instance Learning, Ensemble, Adaboost classifier, Deep Neural Network and the proposed Renyi-Entropy based Cascaded classifier is 72.9, 85.4, 85.6, 87.3 and 88.5, respectively. When the FPR is 80%, the TPR obtained by the existing Multiple Instance Learning, Ensemble, Adaboost classifier, Deep Neural Network and the proposed Renyi-Entropy based Cascaded classifier is 77.7, 88.4, 89.4, 90.5 and 94.3, respectively.

4.4.2. Comparative Analysis using Dataset_2
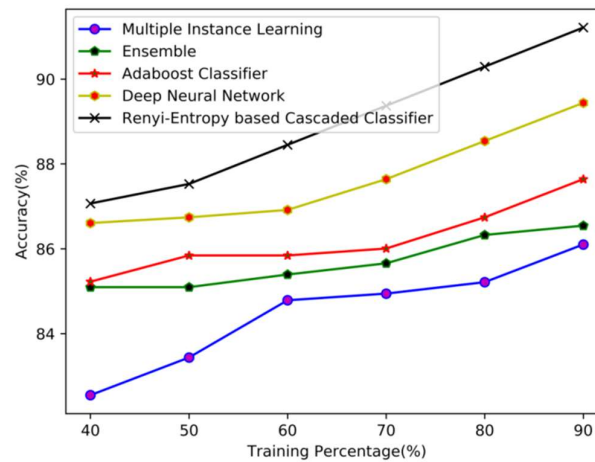
Fig.8. *Comparative Analysis using Accuracy*

Fig.8 shows the comparative analysis using accuracy with respect to the training percentage. When the training percentage is 40, the accuracy obtained by the existing Multiple Instance Learning, Ensemble, Adaboost classifier, Deep Neural Network and the proposed Renyi-Entropy based Cascaded classifier are 82.6, 85.1, 85.2, 86.6 and 87.1, respectively. The accuracy obtained by the existing Multiple Instance Learning, Ensemble, Adaboost classifier, Deep Neural Network and the proposed Renyi-Entropy based Cascaded classifier for the training percentage of 60 is 84.8, 85.4, 85.8, 86.9 and 88.4, respectively. When the training percentage is 90, the accuracy obtained by the existing Multiple Instance Learning, Ensemble, Adaboost classifier, Deep Neural Network and the proposed Renyi-Entropy based Cascaded classifier are 86.1, 86.5, 87.6, 89.4 and 91.2, respectively.
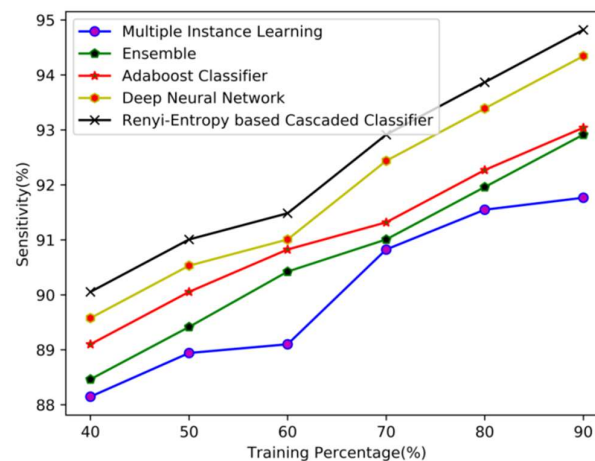
Fig.9.*Comparative analysis using sensitivity*

Fig.9 shows the comparative analysis using sensitivity with respect to the training percentage. The sensitivity obtained by the existing Multiple Instance Learning, Ensemble, Adaboost classifier, Deep Neural Network and the proposed Renyi-Entropy based Cascaded classifier for the training percentage of 40 is 88.1, 88.5, 89.1, 89.6 and 90.1, respectively. When the training percentage is 60, the sensitivity obtained by the existing Multiple Instance Learning, Ensemble, Adaboost classifier, Deep Neural Network and the proposed Renyi-Entropy based Cascaded classifier are 89.1, 90.4, 90.8, 91 and 91.5, respectively. The sensitivity obtained by the existing Multiple Instance Learning, Ensemble, Adaboost classifier, Deep Neural Network and the proposed Renyi-Entropy based Cascaded classifier for the training percentage of 90 is 91.8, 92.9, 93, 94.3 and 94.8, respectively.
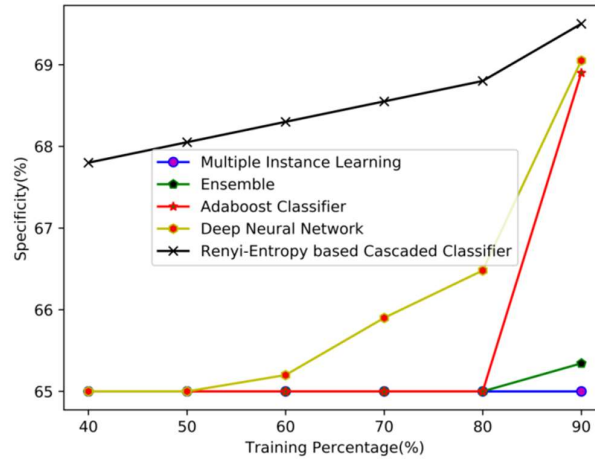
Fig.10. *Comparative Analysis using Specificity*

Fig.10 shows the comparative analysis using specificity with respect to the training percentage. The specificity obtained by the existing Multiple Instance Learning, Ensemble, Adaboost classifier, Deep Neural Network and the proposed Renyi-Entropy based Cascaded classifier for the training percentage of 60 is 65.0, 65.0, 65.0, 65.2 and 68.3, respectively. When the training percentage is 90, the specificity obtained by the existing Multiple Instance Learning, Ensemble, Adaboost classifier, Deep Neural Network and the proposed Renyi-Entropy based Cascaded classifier are 65, 65.3, 68.9, 69.0 and 69.5, respectively.
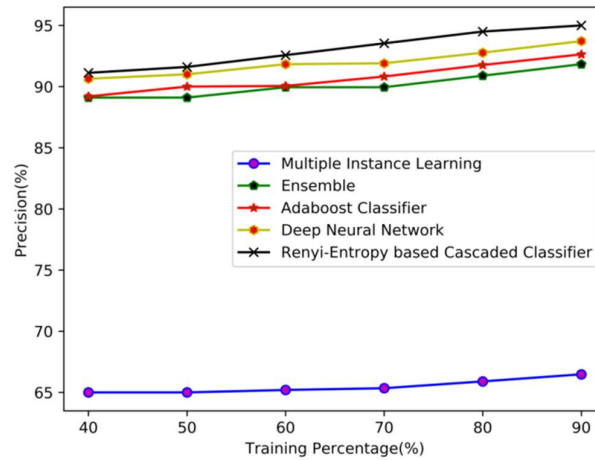
Fig.11. *Comparative Analysis using Precision*

Fig.11 shows the comparative analysis using precision with respect to the training percentage. When the training percentage is 40, the precision obtained by the existing Multiple Instance Learning, Ensemble, Adaboost classifier, Deep Neural Network and the proposed Renyi-Entropy based Cascaded classifier are 65.0, 89.1, 89.2, 90.6 and 91.1, respectively. The precision obtained by the existing Multiple Instance Learning, Ensemble, Adaboost classifier, Deep Neural Network and the proposed Renyi-Entropy based Cascaded classifier for the training percentage of 60 is 65.2, 89.9, 90.1, 91.8 and 92.6, respectively. When the training percentage is 90, the precision obtained by the existing Multiple Instance Learning, Ensemble, Adaboost classifier, Deep Neural Network and the proposed Renyi-Entropy based Cascaded classifier are 66.5, 91.8, 92.6, 93.7 and 95, respectively.
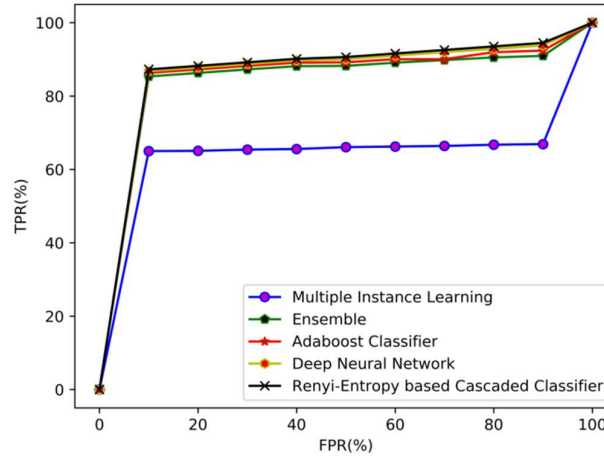
ROC curve:

Fig.12. *ROC curve of Dataset_2*

Fig.12. shows the ROC curve of the dataset_2. The comparative analysis of the proposed Renyi-Entropy based Cascaded classifier with the existing methods in terms of True positive rate (TPR) with respect to the False Positive rate (FPR). When the FPR is 20%, the TPR obtained by the existing Multiple Instance Learning, Ensemble, Adaboost classifier, Deep Neural Network and the proposed Renyi-Entropy based Cascaded classifier is 65.1, 86.3, 87.3, 87.8 and 88.2, respectively. When the FPR is 80%, the TPR obtained by the existing Multiple Instance Learning, Ensemble, Adaboost classifier, Deep Neural Network and the proposed Renyi-Entropy based Cascaded classifier is 66.7, 90.5, 92.0, 92.9 and 93.5, respectively.

4.5 Comparative Discussion

Table 1 shows the comparative discussion using dataset_1. The accuracy of the proposed Renyi-Entropy based Cascaded classifier is, 93.7 which is higher than the existing methods, Multiple Instance Learning, Ensemble, Adaboost classifier, Deep Neural Network which has the accuracy of 86.1, 86.5, 87.6 and 89.4, respectively. The sensitivity obtained by the existing Multiple Instance Learning, Ensemble, Adaboost classifier, Deep Neural Network and the proposed Renyi-Entropy based Cascaded classifier is, 89.4, 90.2, 90.6, 93.5 and 95, respectively. The proposed Renyi-Entropy based Cascaded classifier obtained a specificity of 76.3, when compared to the existing Multiple Instance Learning, Ensemble, Adaboost classifier, Deep Neural Network that provided the specificity of 77, 80.8, 82.3, 84.9, respectively. Table 2 shows the comparative discussion using dataset_2. The precision of the proposed Renyi-Entropy based Cascaded classifier is, 93.7 which is higher than the existing methods, Multiple Instance Learning, Ensemble, Adaboost classifier, Deep Neural Network which has the accuracy of 79.3, 87.8, 89.6, 90.2, 95, respectively.

Table 1: Comparative Discussion using Dataset_1

	Multiple Instance Learning	Ensemble	Adaboost classifier	Deep Neural Network	Renyi-Entropy based Cascaded classifier
Accuracy	85	85.9	86.8	91.2	93.7
Sensitivity	89.4	90.2	90.6	93.5	95
Specificity	76.3	77	80.8	82.3	84.9
Precision	79.3	87.8	89.6	90.2	95

Table 2 shows the comparative discussion using dataset_2. The accuracy of the proposed Renyi-Entropy based Cascaded classifier is,91.2which is higher than the existing methods, Multiple Instance Learning, Ensemble, Adaboost classifier, Deep Neural Network which has the accuracy of 86.1, 86.5, 87.6, and 89.4, respectively. The sensitivity obtained by the existing Multiple Instance Learning, Ensemble, Adaboost classifier, Deep Neural Network and the proposed Renyi-Entropy based Cascaded classifier is, 91.8, 92.9, 93, 94.3 and 94.8, respectively. The proposed Renyi-Entropy based Cascaded

classifier obtained a specificity of 69.5, when compared to the existing Multiple Instance Learning, Ensemble, Adaboost classifier, Deep Neural Network that provided the specificity of 65, 65.3, 68.9, and 69, respectively. Table 2 shows the comparative discussion using dataset_2. The precision of the proposed Renyi-Entropy based Cascaded classifier is, 95 which is higher than the existing methods, Multiple Instance Learning, Ensemble, Adaboost classifier, Deep Neural Network which has the accuracy of 66.5, 91.8, 92.6, and 93.7, respectively.

Table 2: Comparative Discussion using Dataset_2

	Multiple Instance Learning	Ensemble	Adaboost classifier	Deep Neural Network	Renyi-Entropy based Cascaded classifier
Accuracy	86.1	86.5	87.6	89.4	91.2
Sensitivity	91.8	92.9	93	94.3	94.8
Specificity	65	65.3	68.9	69	69.5
Precision	66.5	91.8	92.6	93.7	95

5. Conclusion

A novel DR detection method namely a Renyi-Entropy based Cascaded classifier was developed from the retinal fundus image for detecting the DR. The proposed Renyi-Entropy based Cascaded classifier was developed by combining the Deep RNN, Adaboost classifier, SVM classifier using renyi entropy. Initially, the input image for the detection of DR is subjected to pre-processing for the removal of artifacts from the image. The pre-processed image undergoes the segmentation of optic disc and blood vessel. The segmentation of the blood vessel is performed using the morphological Top-Hat transform and the segmentation of the optic disc is done through the binarization and Circle fixing process. Then, the statistical features, such as mean, variance, standard deviation, energy, and kurtosis and the CNN features are extracted from the optic disc and the blood vessels. Finally, the features extracted are classified by the Renyi-Entropy based Cascaded classifier. When compared with the other state-of-the-arts methods, the proposed Renyi-Entropy based Cascaded classifier obtained a a maximum accuracy of 93.7, maximum precision of 95, maximum sensitivity of 95, and maximum specificity of 84.9, respectively for dataset_1 and obtained a maximum accuracy of 91.2, maximum precision of 95, maximum sensitivity of 94.8, and maximum specificity of 69.5, respectively for dataset_2 respectively.

Compliance with Ethical Standards

Conflicts of interest: Authors declared that they have no conflict of interest.

Human participants: The conducted research follows ethical standards and the authors ensured that they have not conducted any studies with human participants or animals.

References

[1] Zeng, X., Chen, H., Luo, Y. and Ye, W., "Automated Diabetic Retinopathy Detection Based on Binocular Siamese-Like Convolutional Neural Network," IEEE Access, vol.7, pp.30744-30753, 2019.

[2] Pires, R., Avila, S., Jelinek, H. F., Wainer, J., Valle, E., & Rocha, A, " Beyond Lesion-Based Diabetic Retinopathy: A Direct Approach for Referral," IEEE Journal of Biomedical and Health Informatics, vol.21, no.1, pp.193–200, 2017.

[3] Seoud, L., Hurtut, T., Chelbi, J., Cheriet, F., & Langlois, J. M. P, " Red Lesion Detection Using Dynamic Shape Features for Diabetic Retinopathy Screening," IEEE Transactions on Medical Imaging, vol.35, no.4, pp.1116–1126, 2016.

[4] Zhou, L., Zhao, Y., Yang, J., Yu, Q., & Xu, X. ,"Deep multiple instance learning for automatic detection of diabetic retinopathy in retinal images," IET Image Processing, vol.12, no.4, pp.563–571, 2018.

[5] Qummar, S., Khan, F. G., Shah, S., Khan, A., Shamshirband, S., Rehman, Z. U., Jadoon, W, " A Deep Learning Ensemble Approach for Diabetic Retinopathy Detection, " IEEE Access, pp.1–1, 2019.

[6] Costa, P., Galdran, A., Smailagic, A., &Campilho, A., "A Weakly-Supervised Framework for Interpretable Diabetic Retinopathy Detection on Retinal Images," IEEE Access, vol.6, pp.18747–18758, 2018.

[7] Gao, Z., Li, J., Guo, J., Chen, Y., Yi, Z., & Zhong, J. , " Diagnosis of Diabetic Retinopathy Using Deep Neural Networks," IEEE Access, pp.1–1, 2018.

[8] De la Torre, J., Valls, A., & Puig, D., "A Deep Learning Interpretable Classifier for Diabetic Retinopathy Disease Grading," Neurocomputing, 2019.

[9] W. R. Memon, B. Lal, and A. A. Sahto, ``Diabetic retinopathy,'' The Prof. Med. J., vol. 24, no. 2, pp. 234-238, 2017.

[10] S. Haneda and H. Yamashita, ``International clinical diabetic retinopathy disease severity scale,'' Nihon Rinsho. Jpn. J. Clin. Med., vol. 68, pp. 228-235, Nov. 2010.

[11] S. Jan, I. Ahmad, S. Karim, Z. Hussain, M. Rehman, and M. A. Shah, ``Status of diabetic retinopathy and its presentation patterns in diabetics at ophthalomogy clinics,'' J. Postgraduate Med. Inst. (Peshawar-Pakistan), vol. 32, no. 1, pp. 24-27, Mar. 2018.

[12] R. Gargeya and T. Leng, ``Automated identication of diabetic retinopathy using deep learning,'' Ophthalmology, vol. 124, no. 7, pp. 962-969, 2017.

[13] N. Dalal and B. Triggs, ``Histograms of oriented gradients for human detection,'' in Proc. IEEE Comput. Soc. Conf. Comput. Vis. Pattern Recognit. (CVPR), vol. 1, pp. 886-893, Jun. 2005.

[14] D. G. Lowe, ``Object recognition from local scale-invariant features,'' in Proc. ICCV, vol. 2, pp. 1150-1157, Sep. 1999.

[15] T. Ahonen, A. Hadid, and M. Pietikainen, ``Face description with local binary patterns: Application to face recognition,'' IEEE Trans. Pattern Anal. Mach. Intell., vol. 28, no. 12, pp. 2037-2041, Dec. 2006.

[16] J. P. Jones and L. A. Palmer, ``An evaluation of the two-dimensional Gabor filter model of simple receptive elds in cat striate cortex,'' J. Neurophysiol., vol. 58, no. 6, pp. 1233-1258, Dec. 1987.

[17] R. Hazin, M. Colyer, F. Lum, and M. K. Barazi, "Revisiting diabetes 2000: challenges in establishing nationwide diabetic retinopathy prevention programs," American Journal of Ophthalmology, vol. 152, no. 5, pp. 723–729, 2011.

[18] R. Pires, T. Carvalho, G. Spurling, S. Goldenstein, J. Wainer, A. Luckie, H. F. Jelinek, and A. Rocha, "Automated multi-lesion detection for referable diabetic retinopathy in indigenous health care," PLoS ONE, vol. 10, no. 6, 2015.

[19] R. Pires, S. Avila, H. F. Jelinek, J. Wainer, E. Valle, and A. Rocha, "Automatic diabetic retinopathy detection using BossaNova representation," in Intl. Conference of the IEEE Engineering in Medicine and Biology Society, pp. 146–149, 2014.

[20] L. Giancardo, F. Meriaudeau, T. Karnowski, Y. Li, K. Tobin, and E. Chaum, "Microaneurysm detection with radon transform-based classification on retina images," in Intl. Conference of the IEEE Engineering in Medicine and Biology Society, pp. 5939–5942, 2011.

[21] Wang, J.C., Wang, J.F., Lin, C.B., Jian, K.T. and Kuok, W., "Content-based audio classification using support vector machines and independent component analysis," In 18th International Conference on Pattern Recognition (ICPR'06) , vol. 4, pp. 157-160. August 2006.

[22] Mane, V. M., & Jadhav, D. V., "Holoentropy enabled-decision tree for automatic classification of diabetic retinopathy using retinal fundus images," Biomedical Engineering / Biomedizinische Technik, vol.62, no.3, 2017.

[23] DIARETDB0 database from http://www.it.lut.fi/project/ imageret/diaretdb0/.

[24] DIARETDB1 database from http://www.it.lut.fi/project/ imageret/diaretdb1/index.html.

[25] Aswini, S., Suresh, A., Priya, S., & Santhosh Krishna, B. V., "Retinal Vessel Segmentation Using Morphological Top Hat Approach On Diabetic Retinopathy Images," Fourth International Conference on Advances in Electrical, Electronics, Information, Communication and Bio-Informatics (AEEICB), 2018.

[26] V. Vapnik, "Statistical Learning Theory," New York: Wiley, 1998.

[27] Lupascu, C.A., Tegolo, D. and Trucco, E., " FABC: retinal vessel segmentation using AdaBoost," IEEE Transactions on Information Technology in Biomedicine, vol.14, no.5, pp.1267-1274, 2010.

[28] Y. Freund and R. E. Schapire, "A short introduction to boosting," J. Jpn. Soc. Artif. Intell., vol. 14, no. 5, pp. 771–780, Sep. 1999.

[29] Soares, I., Castelo-Branco, M. and Pinheiro, A., "Microaneurysms detection in retinal images using a multi-scale approach", Biomedical Signal Processing and Control, Vol. 79, pp.104184, 2023.

[30] Thanki, R., "A deep neural network and machine learning approach for retinal fundus image classification", Healthcare Analytics, Vol. 3, pp.100140, 2023.

[31] Palaniswamy, T. and Vellingiri, M., "Internet of Things and Deep Learning Enabled Diabetic Retinopathy Diagnosis using Retinal Fundus Images", IEEE Access, 2023.

[32] Sahoo, M., Ghorai, S., Mitra, M. and Pal, S., "Improved Detection Accuracy of Red Lesions in Retinal Fundus Images with Superlearning Approach",Photodiagnosis and Photodynamic Therapy, pp.103351, 2023.

[33] Luo, X., Wang, W., Xu, Y., Lai, Z., Jin, X., Zhang, B. and Zhang, D., "A deep convolutional neural network for diabetic retinopathy detection via mining local and long-range dependence", CAAI Transactions on Intelligence Technology, 2023.

[34] Gu, Z., Li, Y., Wang, Z., Kan, J., Shu, J. and Wang, Q., "Classification of Diabetic Retinopathy Severity in Fundus Images Using the Vision Transformer and Residual Attention", Computational Intelligence and Neuroscience, 2023.

[35] Bajwa, A., Nosheen, N., Talpur, K.I. and Akram, S., "A Prospective Study on Diabetic Retinopathy Detection Based on Modify Convolutional Neural Network Using Fundus Images at Sindh Institute of Ophthalmology & Visual Sciences", Diagnostics, Vol. 13(3), pp.393, 2023.

[36] Jena, P.K., Khuntia, B., Palai, C., Nayak, M., Mishra, T.K. and Mohanty, S.N., "A Novel Approach for Diabetic Retinopathy Screening Using Asymmetric Deep Learning Features", Big Data and Cognitive Computing, Vol. 7(1), pp.25, 2023.